
EXPERIMENTAL DESIGN FOR CAUSAL QUERY ESTIMATION IN PARTIALLY OBSERVED BIOMOLECULAR NETWORKS

A PREPRINT

 **Sara Mohammad-Taheri***

Khoury College of Computer Sciences
Northeastern University
Boston, MA 02115
mohammadtaheri.s@northeastern.edu

 **Vartika Tewari**

Khoury College of Computer Sciences
Northeastern University
Boston, MA 02115
tevari.v@northeastern.edu

 **Rohan Kapre**

Khoury College of Computer Sciences
Northeastern University
Boston, MA 02115
kapre.r@northeastern.edu

 **Karen Sachs**

Next Generation Analytics
Palo Alto, CA
sachskaren@gmail.com

 **Charles Tapley Hoyt**

Laboratory of Systems Pharmacology
Harvard Medical School
Boston, MA
cthoit@gmail.com

 **Jeremy Zucker**

Pacific Northwest National Laboratory
Richland, WA 99354
jeremy.zucker@pnl.gov

 **Olga Vitek**

†
Khoury College of Computer Sciences
Northeastern University
Boston, MA 02115
o.vitek@northeastern.edu

November 30, 2022

ABSTRACT

Estimating a causal query from observational data is an essential task in the analysis of biomolecular networks. Estimation takes as input a network topology, a query estimation method, and observational measurements on the network variables. However, estimations involving many variables can be experimentally expensive, and computationally intractable. Moreover, using the full set of variables can be detrimental, leading to bias, or increasing the variance in the estimation. Therefore, designing an experiment based on a well-chosen subset of network components can increase estimation accuracy, and reduce experimental and computational costs. We propose a simulation-based algorithm for selecting sub-networks that support unbiased estimators of the causal query under a constraint of cost, ranked with respect to the variance of the estimators. The simulations are constructed based on historical experimental data, or based on known properties of the biological system. Three case studies demonstrated the effectiveness of well-chosen network subsets for estimating causal queries from observational data. All the case studies are reproducible and available at https://github.com/srtaheri/Simplified_LVM.

Keywords First keyword · Second keyword · More

*Corresponding author.

†Corresponding author.

1 Introduction

Causal query estimation Pearl [2009] is an essential task in analysis of biomolecular networks. Queries of the form “When we intervene on X , what is the effect on its descendent Y ?” provide insights into the function of biomolecular systems, enable medical decision making, and help develop drugs. Frequently, applying an intervention and collecting interventional data is technologically challenging or expensive. Therefore, methods have been proposed for estimating causal queries from observational data without interventions Jung et al. [2020a,b], Bhattacharya et al. [2020].

Causal query estimation from observational data relies on a known biomolecular network, i.e. a graph where variables (nodes) are signaling proteins, genes, transcripts or metabolites, and directed edges are previously established causal regulatory relationships. Such networks are available in a variety of knowledge bases such as INDRA Bachman et al. [2022], Reactome Gillespie et al. [2022], and Omnipath Türei et al. [2016]. Knowledge-based biomolecular networks are often large, and estimation of causal queries with the entire network can be computationally intractable. Perhaps counterintuitively, using the full set of variables can in fact be harmful, and lead to bias, or increase variance Cinelli et al. [2020]. Therefore, the experimental design should measure a well-chosen subset of variables that minimize the bias and the variance of a causal query estimator.

Additionally, biomolecular measurements incur highly varying costs. For example, while developing a new antibody for flow cytometry experiments is expensive, quantifying a protein with an existing antibody is far cheaper. In mass spectrometry, measurements of low-abundance or modified proteins may require additional steps and incur further costs. Subsets of the transcriptome may be quantified at lower cost than RNA sequencing, using other technologies such as qPCR. Thus, the constraints of measurement costs are an important consideration when designing an experiment.

Existing approaches for selecting a subset of variables for causal query estimation rely on graphical criteria to determine optimal adjustment sets. For example, the adjustment sets include confounders, which, if left unaccounted for, induce spurious correlations. While such criteria are clear for models with no latent variables Rotnitzky and Smucler [2020], Henckel et al. [2019], they have only been established in very restrictive situations for models where latent variables exist Runge [2021]. Moreover, such adjustment sets typically overlook useful variables such as mediators (connecting the cause to the effect via a directed path), and do not consider experimental cost.

In this manuscript, we propose a more comprehensive approach for finding optimal sub-networks, to be quantified in a subsequent observational study, with the objective of minimizing the bias and variance of a causal query estimator under a constraint of measurement cost.

Unlike existing methods that determine optimal adjustment sets based on graphical criteria, we use simulations. Simulations have a long and successful history in computational biology, e.g. single-cell RNA-seq data simulation Cao et al. [2021], Marouf et al. [2020], Sun et al. [2021], stochastic simulation of biochemical reaction systems Marchetti et al. [2017], high-throughput sequencing data simulations (ReSeq) Schmeing and Robinson [2021], and genetic data simulators Peng et al. [2015]. Simulations have been used to model true biological systems accurately, robustly and reproducibly Marouf et al. [2020], in particular in situations with unattainable ground truth Sun et al. [2021], Cao et al. [2021]. They also help in multi-criteria decision making by examining trade-offs Dunke and Nickel [2021].

The proposed approach effectively explores subsets of the variables in the biomolecular network. It uses theoretical considerations, simulation models and sensitivity analysis to characterise the bias and variance of causal query estimators in the presence of latent variables. The simulation-based representation of system variability, and the exploration of broader subsets of variables, allow us to overcome the limitations of techniques that only rely on the adjustment sets. We demonstrate the effectiveness of the proposed algorithm on three Case studies. In the first two, simulation models were constructed based on standard biological practice. In the third, past observational data were used to generate synthetic data with two different strategies, and interventional data were used to verify the validity of the results.

2 Background

2.1 Graphical notation and causal inference

Let boldface letters such as \mathbf{X} be a set of random variables and non-boldface letters such as X be a random variable. Let x be an instance of X , and \mathbf{x} an instance of \mathbf{X} . Let $G = (\mathbf{V} \cup \mathbf{U}, \mathbf{E})$ be a directed acyclic graph (DAG) as in Fig. 1, where \mathbf{V} are observable variables (white nodes), and \mathbf{U} are latent (grey nodes), and \mathbf{E} is a set of edges. Let $P(\mathbf{V})$ be the joint distribution over the observable variables.

An **intervention** (perturbation) on a target variable in the graph (treatment) T fixes it to a constant value t (denoted $do(T = t)$), and makes it independent of its causes [Spirtes et al., 2000, Eberhardt and Scheines, 2007].

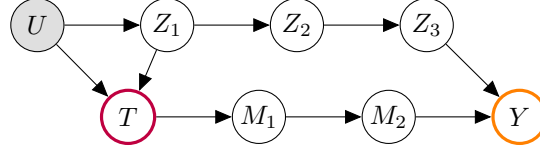


Figure 1: A directed acyclic graph (DAG) with 3 observable confounders (Z_1, Z_2, Z_3) and one latent confounder (U). White nodes are observable and grey nodes are latent. T is the treatment and Y is the effect. M_1 and M_2 are mediators. Y is a collider on the colliding path $M_1 \rightarrow M_2 \rightarrow Y \leftarrow Z_3$.

A **causal query** Q_G over the effect Y is any probabilistic query that conditions on an intervention, such as $Q_G = E[Y|do(T = t)]$ or $E[Y|do(T = 1)] - E[Y|do(T = 0)]$. The latter is a special case of causal query for binary treatments called **average treatment effect (ATE)** Imbens and Rubin [2015]. Such causal queries are the focus of this manuscript. A causal query Q_G is **identifiable** from $P(\mathbf{V})$ compatible with a causal graph G if the query can be computed uniquely Pearl [2009].

A **path** between two variables T and Y exists if there is a sequence of edges connecting T to Y . A **directed path** follows the direction of the edges. A **causal path** from T to Y is a directed path from T to Y . Let $cp(T, Y, G)$ be all the variables on causal paths from T to Y in G excluding T . E.g. in Fig. 1, $cp(T, Y, G) = \{M_1, M_2, Y\}$. The **mediators** are all the variables on $cp(T, Y, G)$ except T and Y .

d-separation Pearl [2009] captures true independencies (i.e., separations) in a path. A path p is d-separated (or blocked) by a set of variables \mathbf{Z} if and only if,

- p contains a chain $V_i \rightarrow V_j \rightarrow V_k$ or a fork $V_i \leftarrow V_j \rightarrow V_k$ such that the middle variable V_j is in \mathbf{Z} , or
- p contains a collider $V_i \rightarrow V_j \leftarrow V_k$ such that the middle variable V_j is not in \mathbf{Z} and such that no descendant of V_j is in \mathbf{Z} .

A set \mathbf{Z} d-separates T from Y if and only if \mathbf{Z} blocks every path from T to Y . For example in Fig. 1, any subset of $\{Z_1, Z_2, Z_3\}$ blocks the path $T \leftarrow Z_1 \rightarrow Z_2 \rightarrow Z_3 \rightarrow Y$.

In order to quantify the direct effect of T on Y , one must isolate the effect of any possible confounders. A **confounder** is a variable that affects both T and Y . E.g., in Fig. 1, Z_1, Z_2 , and Z_3 are confounders. A path with arrows coming into both T and Y is called a **backdoor path**. In Fig. 1 $T \leftarrow Z_1 \rightarrow Z_2 \rightarrow Z_3 \rightarrow Y$ is a backdoor path. The easiest way to eliminate confounding is to block all backdoor paths.

Frequently, some variables in a DAG are unobserved (i.e., latent) such as U in Fig. 2(a). DAGs with latent variables are compactly represented by **acyclic directed mixed graphs (ADMGs)** Richardson et al. [2017] such as in Fig. 2(c). An ADMG $\mathcal{G} = (\mathbf{V}, \mathbf{E}_d, \mathbf{E}_b)$ consists of a set of observable variables \mathbf{V} , a set of directed edges \mathbf{E}_d , and bidirected edges \mathbf{E}_b . A bidirected edge indicates a path including any number of latent variables without colliders that point to two observable variables. ADMGs allow us to misspecify the number and type of the latent variables, as long as we accurately represent the topology over the observed variables. ADMG is the main graph structure in this manuscript.

An ADMG is constructed by using the following **simplification rules** Evans [2016]:

1. Remove latent variables with no children from the graph. E.g., U_5 in Fig. 2(a) is removed in Fig. 2(b).
2. Transform a latent variable with parents to an exogenous variable where all its parents are connected to its children. E.g., U_3 in Fig. 2(a) and (b).
3. Remove an exogenous latent variable that has at most one child. E.g., U_4 in Fig. 2(a) is removed in Fig. 2(b).
4. If U, W are latent variables where children of W are a subset of children of U , then, W can be removed. E.g., U_1 and U_2 in Fig. 2(a), and U_2 is removed in Fig. 2(b).

2.2 Input variables for causal query estimators

Given an ADMG and a causal query of interest, our objective is to determine which variables in the DAG should be used as input to a causal query estimator. The choice of the variables determines the estimator’s bias and variance. An estimator is **biased** if it systematically deviates from its true value. **Variance** of the estimator is its variability across repeatedly collected datasets.

The set of variables blocking the backdoor paths is called a **valid adjustment set** (e.g., $\{Z_1, Z_2, Z_3\}$ in Fig. 1). The smallest set of variables that block all the back-door paths is called a **minimal adjustment set** (e.g., Z_1 or Z_2 or Z_3 in Fig. 1). However, different adjustment sets produce estimators with different variance.

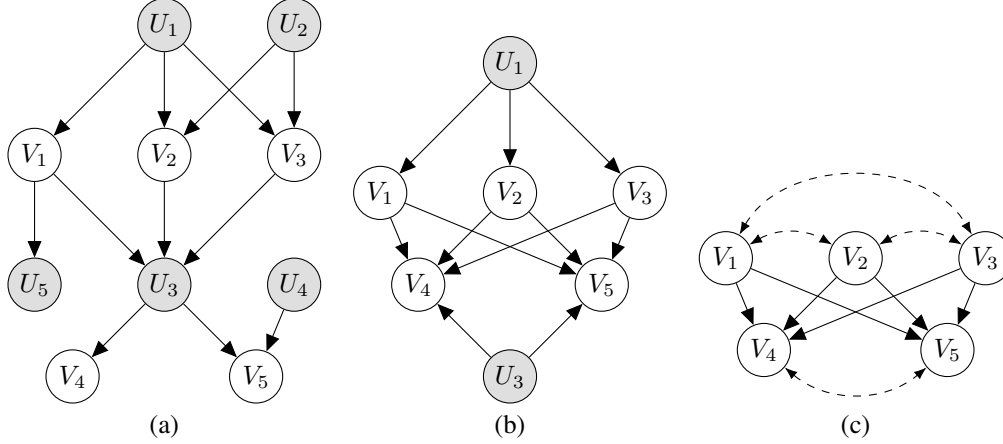


Figure 2: (a) DAG G . White nodes are observable and grey nodes are unobserved (latent). (b) Simplified sub-DAG \tilde{G} according to simplification rules. (c) Corresponding ADMG \mathcal{G} . Bi-directed edges show presence of latent variable. The exact number and structure of latent variables in an ADMG can be misspecified.

A minimal subset of the variables that blocks all back-door paths and maximally reduces the variability in Y is an **optimal adjustment set** (e.g., Z_3 in Fig. 1). In absence of latent variables, the optimal adjustment set $O(T, Y, G)$ is defined as [Rotnitzky and Smucler, 2020]

$$O(T, Y, G) = Pa(cp(T, Y, G)) \setminus (de(cp(T, Y, G)) \cup T) \quad (1)$$

Here $Pa(cp(T, Y, G))$ are the parents, and $de(cp(T, Y, G))$ are the descendants of all the variables in $cp(T, Y, G)$. A valid, minimal, or optimal adjustment set can be computed with open-source R packages such as `pcaIlg` Kalisch et al. [2012], `dagitty` Textor et al. [2016], and `causalEffect` Tikka and Karvanen [2017].

In presence of latent variables, Runge [2021] showed that an optimal adjustment set exist in the specific case of linear models and under specific conditions. Beyond that, an optimal adjustment set does not exist in most scenarios. However, Cinelli et al. [2020] provided graphical guidelines for determining adjustment sets that do not cause bias and possibly reduce or increase variance, as follows.

Bad controls, when added to the adjustment set, increase the bias of the query estimators. These variables (1) open a backdoor path between T and Y (i.e. are colliders), (2) are mediators or children of the mediators, (3) open a path that contains a collider between T and Y , (4) are in $de(Y)$.

Neutral controls, when added to the adjustment set, neither increase nor decrease the bias, but may either increase or decrease the variance of the estimators. **Good neutral controls** are possibly good for precision. These are variables that (1) when added to the adjustment set, do not undermine the identifiability of the query, and (2) are in $O(T, Y, G)$. **Bad neutral controls** are possibly bad for precision. These are variables that 1) not necessary for the identifiability of the query, and 2) are in $Pa_G(T)$ Hahn [2004], White and Lu [2011], Henckel et al. [2019].

2.3 Existing causal query estimators

Given an ADMG, and a causal query of interest, the next objective is to choose an estimator for the query. Many estimators are implemented in open-source libraries such as DoWhy Sharma et al., Ananke Bhattacharya et al. [2020], and the Y_0 engine Zucker and Hoyt [2021]. In this manuscript we focus on the following.

Non-parametric and semi-parametric estimators such as gformula, inverse probability weight (IPW), augmented IPW (AIPW), Nested IPW and augmented nested IPW [Bhattacharya et al., 2020] are all implemented and well-documented in Ananke. These estimators are asymptotically unbiased, do not require parametric assumptions, and are computationally cheap. However, they are limited to causal queries with one treatment and one effect, and the treatment must be binary-valued. Moreover, they limit the variables used for query estimation. For example, the IPW estimator only uses the cause, effect and a valid adjustment set. The rest of variables such as mediators and the variables not in the adjustment set are ignored.

Causal generative models expand causal query estimation beyond a single binary treatment and a single effect. Mohammad-Taheri et al. [2022] represented the data generating process with a directed graphical model. The approach

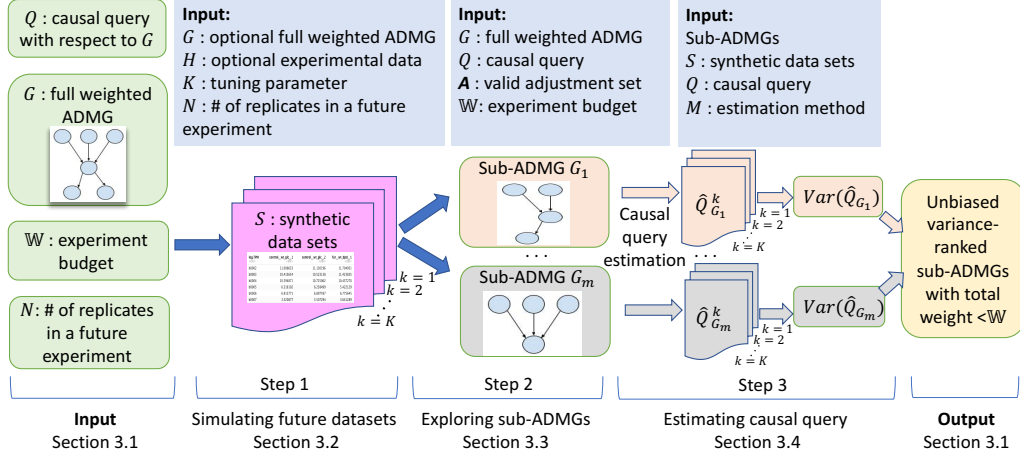


Figure 3: Overview of the proposed approach. Arrows indicate sequence of steps. Inputs specific to the biological problem are shown in green. Additional tuning parameters and analytical options specified for each step are shown in blue.

1) estimates the posterior distribution over the model parameters given the training data, 2) fixes the targets of the intervention, and breaks their relationship to their parents, and 3) samples the parameters from their posterior distributions, and then samples from each variable given its parents. The estimator can be thought of as a posterior predictive statistic over the marginal of the parameters. The query is estimated in an asymptotically unbiased manner with all the variables, except for the ancestors of the treatment T that do not affect the descendants of T , and except for the descendants of the effect. Unfortunately, the approach is computationally expensive and requires parametric assumptions.

Linear regression without mediators simplifies the complexity of causal generative models by only regressing T and adjustment set on Y . The coefficient of T is an unbiased estimator of the ATE. For example in Fig. 1,

$$Y = \beta_0 + \beta T + \gamma Z_i + \epsilon; \epsilon \stackrel{iid}{\sim} \mathcal{N}(0, \sigma^2) \quad (2)$$

The least squares estimator $\hat{\beta}$ estimates the ATE of T on Y without bias. Even after adding more than one Z_i , $i \in \{1, 2, 3\}$ the estimator of the ATE remains unbiased because the backdoor path remains blocked. However its variance will change. $E[Y|do(T = t)]$ is estimated by substituting $\hat{\beta}$ and $\hat{\gamma}$ in Eq. (2) and averaging over the values of Y .

The linear regression without mediators approach is simple, fast, and highly interpretable. It takes as input treatment, effect and any variables in the adjustment set. However, it is only appropriate when the variables are linearly related.

Linear regression with mediators allows for inclusion of mediators absent from an adjustment set. Similarly to linear regression without mediators, it estimates the ATE of V_i on V_j for any pair of variables on the causal paths between T and Y , and multiply all the estimated ATEs. In Fig. 1,

$$M_1 = \alpha_0 + \alpha T + \nu; \nu \stackrel{iid}{\sim} \mathcal{N}(0, \sigma_\nu^2) \quad (3)$$

$$M_2 = \rho_0 + \rho M_1 + \psi; \psi \stackrel{iid}{\sim} \mathcal{N}(0, \sigma_\psi^2) \quad (4)$$

$$Y = \eta_0 + \eta M_2 + \delta Z_i + \omega; \omega \stackrel{iid}{\sim} \mathcal{N}(0, \sigma_\omega^2) \quad (5)$$

By substituting Eq. (3) into Eq. (4), and Eq. (4) into Eq. (5)

$$Y = \eta_0 + \eta\rho_0 + \eta\rho\alpha_0 + (\eta\rho\alpha)T + \delta Z_i + \eta\rho\nu + \eta\psi + \omega = \zeta_0 + \zeta T + \delta Z_i + \epsilon' \quad (6)$$

where $\epsilon' \stackrel{iid}{\sim} \mathcal{N}(0, \eta^2\rho^2\sigma_\nu^2 + \eta^2\sigma_\psi^2 + \sigma_\omega^2)$. We establish that $\eta\rho\alpha$ is an ATE, and that the least squares estimator of $\eta\rho\alpha$ is unbiased. Estimating η , ρ and α separately and multiplying the estimates reduces the variance of the estimator Bellemare et al. [2019].

2.4 Simulation-based inference

Synthetic data representative of a particular experiment is an increasingly popular strategy for experiment planning and analysis. Generative models such as GANs Goodfellow et al. [2020] successfully generated high-quality artificial genomes Yelmen et al. [2019], MRI scans Pawlowski et al. [2020], and electronic health records while mitigating privacy concerns Choi et al. [2017], Weldon et al. [2021].

Numerous single-cell RNA (scRNA-seq) sequencing data simulation methods Marouf et al. [2020] have been developed to generate realistic scRNA sequencing data, and to produce data with desired structure (such as specific cell types or subpopulations) while preserving genes, capturing gene correlations, and generating any number of cells with varying sequencing depths Cao et al. [2021], Sun et al. [2021]. They were also useful to augment sparse cell populations and improve the quality and robustness of downstream classification. To the best of our knowledge, there are currently no approaches for simulation-based design of experiments for causal query estimation.

3 Methods

We propose an approach that assists with planning a future experiment for causal query estimation. We combine the existing methods for finding optimal adjustment sets, and synthetic data generation. We report sub-ADMGs supporting (asymptotically) unbiased estimation of a causal query, and ranked according to variance of the causal query estimator and experimental cost. The user can select for future measurement a sub-ADMG that balances variance of the query and cost. Fig. 3 overviews the approach.

3.1 Input and output

The proposed approach takes as input a weighted ADMG G from a knowledge base such as INDRA or Omnipath. The ADMG can misspecify the structure of the latent variables, as long as it accurately represents the structure over the observable variables. The observable variables of the ADMG are weighted by their associated experimental cost.

The proposed approach also takes as input a causal query Q with respect to G of the form $E[Y|do(T = t)]$ or $ATE = E[Y|do(T = t + 1)] - E[Y|do(T = t)]$ for a given t , the upper limit on the experimental budget \mathbb{W} , and the number of replicates N in the experiment being planned.

The proposed approach outputs a list of sub-ADMGs G_1, \dots, G_m that support asymptotically unbiased estimation of the query and satisfy the budget constraint. The sub-ADMGs are ranked by the empirically evaluated variance of the causal query estimators.

3.2 Step 1 : Simulating future data sets

The approaches in Sec. 2.2 that determine input variables for causal query estimation have limitations. They focus on graphical criteria, and do not consider variables such as mediators that can't be part of an adjustment set. Furthermore, in presence of latent variables no uniformly optimal adjustment set may exist Henckel et al. [2019], Rotnitzky and Smucler [2020]. Therefore, we evaluate the estimators by generating K synthetic datasets that mimic the future experiment, with N observations each. The methodological challenges are the choice of the simulator, and the diagnostics of the simulation accuracy. K is a tuning parameter.

When historical experimental data (e.g., prior data from the same organism, or from related systems or technologies) exist, the synthetic data is constructed based on approaches such as Tabular GAN Xu et al. [2019], or based on statistical associations such as Bayesian network forward simulation Koller and Friedman [2009]. The latter requires as input the knowledge of the ADMG. The quality of the synthetic data is evaluated by comparing the marginal and the joint distributions of the synthetic and the experimental data. In absence of historical data, the synthetic data sets are constructed using reasonable or known ranges for model parameters, and functional forms such as Hill equations Alon [2019]. The quality is evaluated by sensitivity analysis across multiple values of parameters and functional forms.

3.3 Step 2 : Exploring sub-ADMGs

Description of the algorithm This step generates sub-ADMGs that support (asymptotically) unbiased estimation of the causal query and do not exceed the budget. The biological inputs to the step are the full weighted ADMG, the causal query of interest, and the experimental budget. The technical input is a valid adjustment set that includes all the good neutral controls that are proven to possibly decrease the variance of the estimation. Algo 2 in Appendix describes the generation of the adjustment set. We call the treatment, effect, and the adjustment set the **required variables**, necessary

for an (asymptotically) unbiased estimation of the query. These variables are always present in the search space. The rest of (yet unexplored) variables are **optional nodes**.

The remainder of Step 2 is detailed in Algo 1. Since unidentifiable queries provide biased estimators, the algorithm raises an error if the input query is unidentifiable (line 1). Descendants of Y (i.e., bad controls in Sec. 2.2) can't cause any variation in Y , and also bias the results. Hence, we only consider the ancestral graph of Y (line 4).

The algorithm iterates over subsets of nodes in the ancestral graph limited to those which contain all the required nodes and have sum of weights less than the given budget (line 6, Algo 3 and Algo 4 in Appendix). For each of these subsets a sub-ADMG is generated (line 7, Algo 5 in Appendix).

Properties of the algorithm Algo 1 enumerates all the sub-ADMGs satisfying the budget constraint, and finds the sub-ADMG(s) with globally minimal variance of the causal query estimator. Lemma 1 in Appendix shows that including any number of mediators as input to the causal query estimator always reduces the variance. Therefore, the optimal sub-ADMG always includes mediators.

Algo 1 is of exponential complexity. For $\mathbb{W} = \infty$, the running time complexity is of the order of $O(n \times 2^n)$, where n is the total number of optional variables. Setting $\mathbb{W} < \infty$ limits the search space and reduces the complexity.

Despite the exponential complexity, Algo 1 supports many practically relevant queries. The case studies in this manuscript took between 2 to 10 minutes on a parallel Google cloud Platform with 2 vCPUs and 8 GB memory.

For large-scale problems, we can take additional shortcuts. As we show in the Case studies, a single mediator substantially decreases the variance of the causal query estimator. For every additional mediator the decrease is smaller. Therefore, searching over sub-ADMGs with a single mediator can be effective. Another shortcut is to stop the algorithm once the selected variables reduce the variance with respect to the required variables by a pre-specified amount. These shortcuts do not produce globally optimal sub-ADMGs, but reduce the experimental and computational cost.

Algorithm 1: generateSetOfRankedSubADMGs

Input: $\mathcal{G} = (\mathbf{V}, \mathbf{E}_d, \mathbf{E}_b, \mathbf{W})$: Weighted ADMG

T, Y : Treatment and effect variables

$Q_{\mathcal{G}}$: Causal query

\mathbf{A} : A valid adjustment set //Output of Alg7 in Appx

\mathbf{D} : Input data sets // Step 1

M : Causal query estimator

Parameter: \mathbb{W} : Upper limit on the total weight

Output: A set of variance-ranked sub-ADMGs with total weight $\leq \mathbb{W}$. T, Y and \mathbf{A} are always present.

```

1 if  $Q_{\mathcal{G}}$  is not identifiable then
2   | raise not identifiable error
3 end
4  $\mathcal{G} \leftarrow \mathcal{G}_{an(Y)}$  // Ancestral graph of  $Y$ 
5 subADMGSet  $\leftarrow \{\}$ 
6 for  $s \in \text{getValidNodeSubsets}(\mathcal{G}, \mathbf{A}, T, Y, \mathbb{W})$  do
7   |  $\mathcal{G}' = \text{generateSubADMG}(\mathcal{G}, s)$  //Step 2
8   |  $\hat{Q}_{\mathcal{G}} = \text{estimateQuery}(\mathcal{G}', Q_{\mathcal{G}}, \mathbf{D}, M)$  //Step 3
9   | subADMGSet.add $\{\mathcal{G}' : \text{var}(\hat{Q}_{\mathcal{G}})\}$ 
10 end
11 return sorted subADMGSet based on variance

```

3.4 Step 3 : Estimating causal query

This step estimates the query for each sub-ADMG over all the K synthetic data sets (Algo 1, line 8). The technical input is the choice of a query estimator. Here we consider all the estimators in Sec. 2.3. For the semi- and non-parametric approaches, Algo 1 only searches over the variables that these estimators use and disregard the rest. Finally, we calculate the empirical variance for each sub-ADMG (Algo 1, line 9). When Algo 1 repeated with different causal query estimators and different number of replicates N , we can evaluate the impact of the sample size and of the estimator.

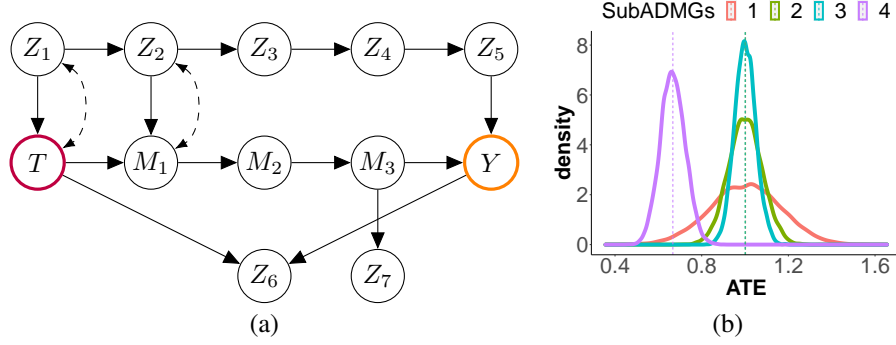


Figure 4: **Illustrative example** (a) The full ADMG, with treatment T and effect Y . The minimal adjustment set is Z_1 and the optimal adjustment set is $\{Z_1, Z_2, Z_5\}$. (b) ATE density for linear regression estimates on over 10000 data sets for a selection of sub-ADMGs in Sec. 3.5, Step 2. True ATE=1. The optimal **Sub-ADMG 3** consists of $T, Y, Z_1, Z_2, Z_5, M_1, M_2$. Estimate of ATE with the full ADMG (**Sub-ADMG 4**) biased the results.

3.5 Illustrative example

This simple example illustrates the impact of using a subset of variables to measure on a causal query estimation, in an idealized case where the data generation process is known.

Ground truth Consider the weighted ADMG in Fig. 4, where T is the treatment and Y is the effect. The causal query of interest is the ATE. Denote \mathbf{X} the set of all the variables. Assume that the data generation process follows,

$$X = \theta Pa(X) + N_X; N_X \stackrel{iid}{\sim} \mathcal{N}(0, 1) \quad (7)$$

with $\theta = 1$. Since the ATE is the coefficient of T , when T and the adjustment sets are regressed on Y , the true ATE=1.

Input Assume that the proposed approach takes as input the correct ADMG in Fig. 4, T, Y , and the query ATE. Assume that all the variables have the same cost of 1 (i.e., the total cost is the number of variables), $\mathbb{W} = \infty$, and $N = 500$.

Step 1: Simulating future data sets We generated 10000 synthetic data sets with 500 data points from Eq. (7).

Step 2: Exploring sub-ADMGs In this example the minimal valid adjustment set is Z_1 , i.e. Z_1 is always present in the search space. We hand-picked 4 sub-ADMGs that illustrate the proposed approach. They consist of,

- 1) **Sub-ADMG 1:** T, Y, Z_1
- 2) **Sub-ADMG 2:** T, Y, Z_1, Z_2, Z_5
- 3) **Sub-ADMG 3:** $T, Y, Z_1, Z_2, Z_5, M_1, M_2, M_3$
- 4) **Sub-ADMG 4:** full ADMG in Fig. 4 (a).

Step 3: Estimating causal query For each simulated data set and each sub-ADMG, we estimated the ATE. With the first sub-ADMG, the ATE is estimated by controlling for the effect of the confounders by blocking the backdoor path between T and Y by adjusting for Z_1 ,

$$Y = \beta T + \zeta Z_1 + \epsilon; \epsilon \stackrel{iid}{\sim} \mathcal{N}(0, 1) \quad (8)$$

Here $\widehat{ATE} = \hat{\beta}$ is an unbiased estimator. With the second sub-ADMG, the ATE is estimated by controlling for the effect of the confounders by blocking the backdoor path with Z_1 while also including Z_2, Z_5 .

$$Y = \delta T + \eta Z_1 + \kappa Z_2 + \phi Z_5 + \nu; \nu \stackrel{iid}{\sim} \mathcal{N}(0, 1) \quad (9)$$

Note that Z_2 and Z_5 are good neutral controls. In this case, $\widehat{ATE} = \hat{\delta}$ is unbiased and has smaller variance.

With the third sub-ADMG, the query is estimated by including the mediators (M_1, M_2, M_3):

$$M_1 = \alpha T + \gamma Z_1 + \psi Z_2 + \omega; \omega \stackrel{iid}{\sim} \mathcal{N}(0, 1) \quad (10)$$

$$M_2 = F M_1 + \varphi; \varphi \stackrel{iid}{\sim} \mathcal{N}(0, 1) \quad (11)$$

$$M_3 = \rho M_2 + \varrho; \varrho \stackrel{iid}{\sim} \mathcal{N}(0, 1) \quad (12)$$

$$Y = \chi M_3 + \varkappa Z_5 + \varepsilon; \varepsilon \stackrel{iid}{\sim} \mathcal{N}(0, 1) \quad (13)$$

Here $\widehat{ATE} = \hat{\alpha} \hat{F} \hat{\rho} \hat{\chi}$ is unbiased estimator of ATE and the estimate has a smaller variance than the first two approach. With the fourth sub-ADMG, the ATE is estimated by including all the variables into estimation of the query.

Output and conclusions Fig. 4 (b) shows the results of query estimation over the synthetic data for each sub-ADMG. We can make several conclusions. (1) As expected, the adjustment set that included the good neutral controls (Z_2, Z_5) reduced the variance compared to only measuring the minimal adjustment set (Z_1). (2) Including the mediators reduced the variance beyond what was possible with the adjustment set. Mediators are often viewed as bad controls, and not used for causal query estimation. This example illustrated that mediators can reduce the variance of estimators, at least in a linear setting. (3) Using all the variables was detrimental. Since some of the included variables were bad controls (Z_6, Z_7), they biased the results.

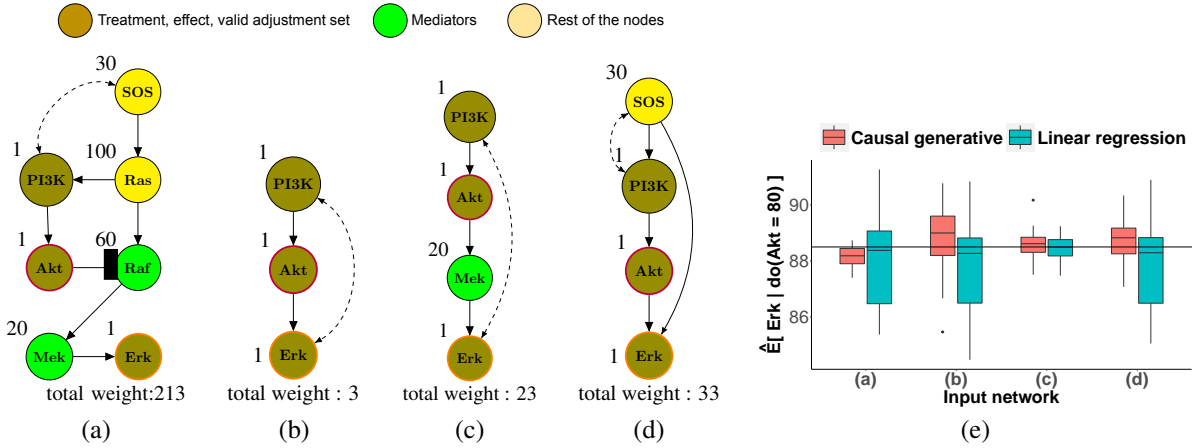


Figure 5: **Case study 1.** (a) Full weighted ADMG. *Akt* is the treatment and *Erk* is the effect. Bi-directed edges indicate presence of latent variables. (b)-(d) Example sub-ADMGs. Simplification rules in Sec. 2.1 lead Algo 1 to convert the latent variables into exogenous variables, shown with bi-directed edges. (e) Sampling distribution of $\hat{E}[Erk | do(Akt = 80)]$ over $K = 20$ simulated observational data, $N = 100$. The horizontal line is the true value of the query from interventional data. The apparent bias was due to the approximations in the model assumptions, and to the asymptotic nature of the estimators.

Variance by	N = 20				N = 100			
	Fig. 5(a)	Fig. 5(b)	Fig. 5(c)	Fig. 5(d)	Fig. 5(a)	Fig. 5(b)	Fig. 5(c)	Fig. 5(d)
Linear regression	21.72	18.40	1.67	19.78	2.39	2.41	0.236	2.25
Causal generative	1.22	4.83	0.75	6.95	0.15	1.60	0.33	0.66

Table 1: **Case study 1.** Impact of the choice of the estimator, and of N . Highlighted cells show minimal variance.

4 Case studies of biomolecular networks

We illustrate the practical utility of the proposed algorithm in three Case studies with a broad set of network topologies, causal query types, synthetic data generation approaches and causal query estimators. In particular, Case study 3 was based on observational experimental measurements of *E. Coli*, and was validated using interventional experimental measurements. The causal generative approach was implemented with RStan [Stan Development Team, 2020]. More details, including model formulas, are in Appendix.

4.1 Case study 1: The IGF signalling pathway

Input Fig. 5 (a) shows the full weighted ADMG of the insulin growth factor (IGF) signaling system, regulating growth and energy metabolism of a cell. Variables are kinase proteins, and pointed/flat-headed edges represent the effect (increase/decrease) of the upstream kinase on the downstream kinase’s activity. Assume that the costs of measuring each variable is 100 for *Ras*, 60 for *Raf*, 20 for *Mek*, 30 for *SOS*, and $\mathbb{W} = 50$. The causal query of interest is $E[Erk|do(Akt = 80)]$, and $N = 100$.

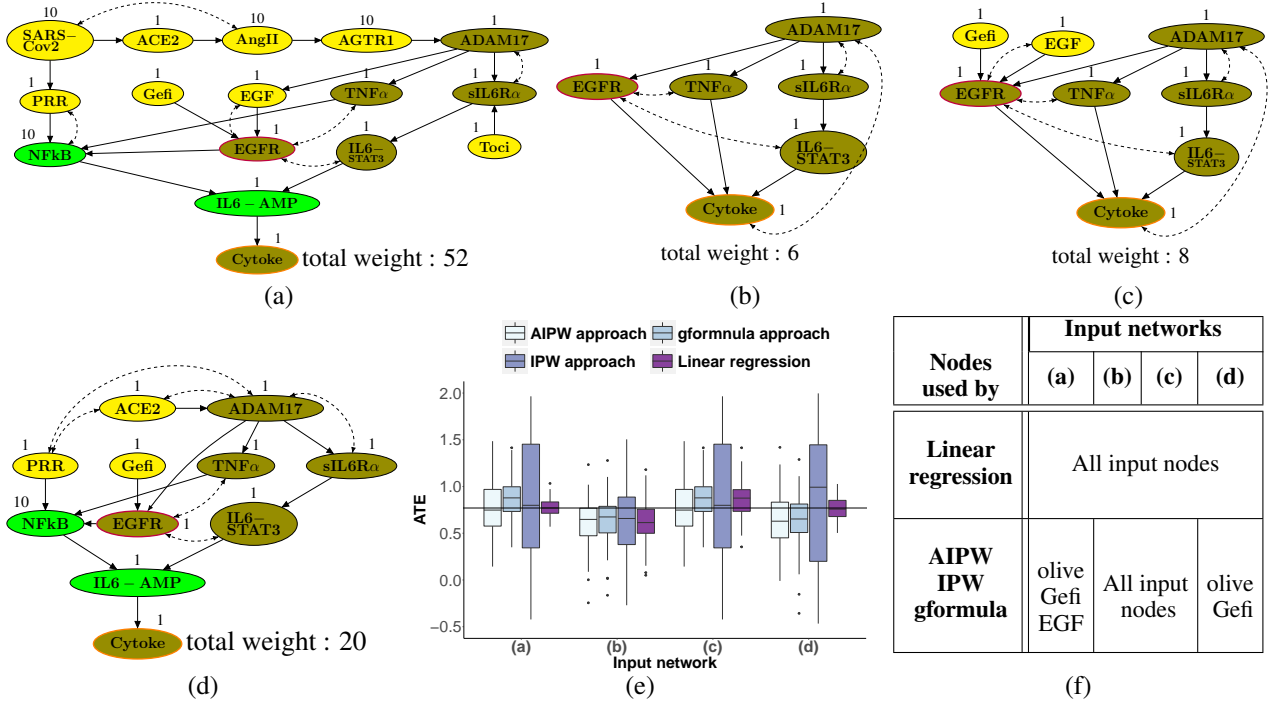


Figure 6: **Case study 2.** (a) Full weighted ADMG. Node colors are as in Fig. 5. *EGFR* is the treatment and *CytokineStorm* is the effect. Bi-directed edges indicate presence of latent variables. (b)-(d) Example Sub-ADMGs. Simplification rules in Sec. 2.1 lead Algo 1 to convert the latent variables into exogenous variables, shown with bi-directed edges. (e) Sampling distribution of $ATE = E[CS|do(EGFR = 1)] - E[CS|do(EGFR = 0)]$ over $K = 100$ simulated data, $N = 1000$. The horizontal line is the true ATE from interventional data. The apparent bias was due to the approximations in the model assumptions, and to the asymptotic nature of the estimators. (f) Variables used by different query estimators.

Step 1: Simulating future data sets Since IGF dynamics is well characterized in form of stochastic differential equations (SDE), we did not use any historical data. Instead, we generated $K = 20$ observational datasets by simulating from the SDE. We set the initial amount of each protein to 100, and generated subsequent observations via the Gillespie algorithm Gillespie [1977] with the *smfsb* Wilkinson et al. [2018] R package. To evaluate the true value of the query, we simulated interventional data while fixing $Akt = 80$.

Step 2: Exploring sub-ADMGs Fig. 5(a)-(d) shows some sub-ADMGs explored by Algo 1. Since $\{PI3K\}$ was a valid adjustment set, it always remained in the search space together with the treatment (Akt) and the effect (Erk). *Ras* and *Raf* were absent as their cost exceeded \mathbb{W} .

Step 3: Estimating causal query The non-parametric and semi-parametric estimation approaches were not applicable to the continuous treatment Akt . Hence, we used the causal generative and the linear regression estimation approaches.

Output and conclusions Fig. 5(e) summarizes the queries estimated over $K = 20$ simulated observational datasets. We can make several conclusions. 1) Including a single mediator in Fig. 5(c) to the adjustment set of olive nodes in Fig. 5(b) reduced the variance of the causal query estimator by over 50% (Table 1); 2) Using the full network in Fig. 5(a) was suboptimal. Other sub-ADMGs had a comparable variance and lower cost (Table 1); 3) The choice of estimator and of N affected the ranking of sub-ADMGs (Table 1).

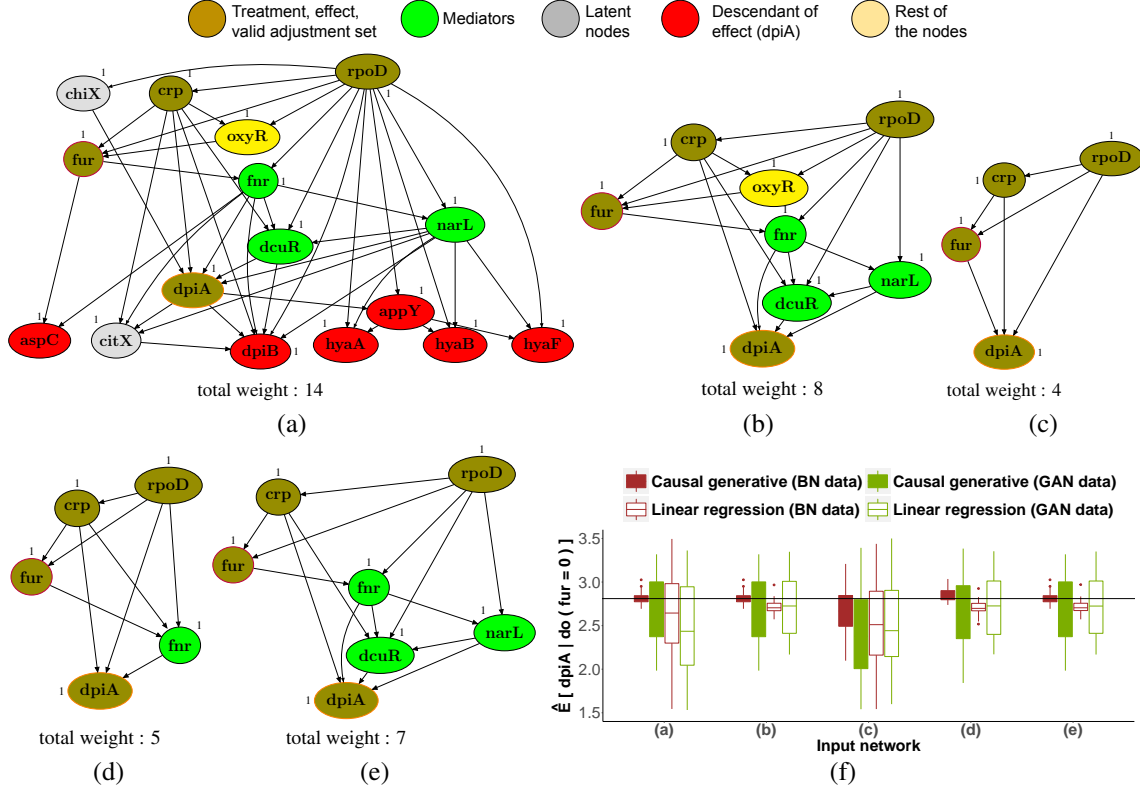


Figure 7: **Case study 3.** (a) Full weighted ADMG. *fur* is the treatment and *dpia* is the effect. (b) Algo 1 removed the red and grey nodes from the search space. (c)-(e) Example sub-ADMGs. Simplification rules in Sec. 2.1 lead Algo 1 removing the latent variables. (f) Sampling distribution of $Q_{fur} = P(dpia | do(fur = 0))$ estimation over $K = 100$ simulated data, $N = 1000$. The horizontal line is true value obtained experimentally, upon an intervention. The apparent bias was due to the approximations in the model assumptions, and to the asymptotic nature of the estimators.

4.2 Case study 2: The SARS-CoV-2 model

Input The full weighted ADMG in Fig. 6(a) models activation of Cytokine Release Syndrome (cytokine storm), known to cause tissue damage in severely ill SARS-CoV-2 patients Ulhaq and Soraya [2020]. The simultaneous activation of the nuclear factor kappa-light-chain-enhancer of activated B cells (NF- κ B) and Interleukin 6-STAT3 Complex (IL6-STAT3) initiates a positive feedback loop known as Interleukin 6 Amplifier (IL6-AMP), which in turn activates Cytokine Storm Hirano and Murakami [2020]. Gefitinib (Gefi) is an immunosuppressive drug that blocks epidermal growth factor receptor (EGFR), and prevents the cytokine storm. The causal query examines the $ATE = E[CS | do(EGFR = 1)] - E[CS | do(EGFR = 0)]$. $\mathbb{W} = \infty$, and $N = 1000$.

Step 1: Simulating future data sets For this case study, the generation of synthetic data was motivated by common biological practice. Simple biomolecular reactions were modeled with Hill function Alon [2019] as $\mathcal{N}(\frac{100}{1 + \exp(\theta' Pa(X) + \theta_0)}, \sigma_X)$, where $Pa(X)$ is a $q \times 1$ vector of measurements on the parent of X , θ' is a $1 \times q$ vector of parameters, and θ_0 is a scalar. Probability distributions of the exogenous variables were simulated as $\mathcal{N}(\mu_r, \sigma_r)$. The treatment $EGFR$ was binary. Interventional data were generated similarly, while fixing $EGFR$ to 1 and 0, and were used to define the true value of the query. $K = 100$.

Step 2: Exploring sub-ADMGs Fig. 6(a)-(d) shows some sub-ADMGs explored by Algo 1. The adjustment set, the treatment and the effect (olive nodes) were always present.

Step 3: Estimating causal query Since the treatment is single and binary, we considered the semi- and non-parametric approaches in Ananke (AIPW, IPW, and gformula), and the linear regression. RStan was unable to fit a causal generative approach with a discrete variable.

Output and conclusions Fig. 6(e) summarizes the queries estimated over $K = 100$ simulated observational data sets. We can make several conclusions. 1) For linear regression, the full network in Fig. 6(a) and the sub-network in Fig. 6(d)

had similar variances, but at different cost. 2) For linear regression, compared to using the adjustment set alone in Fig. 6(b), including mediators in Fig. 6(d) reduced the variance of the query estimation. However, this was not the case for AIPW, IPW, and gformula estimators, as they were constrained to certain input variables regardless of the input (Fig. 6(f)). 3) For AIPW, IPW, and gformula, the full network in Fig. 6(a) and the sub-network in Fig. 6(c) had exact same results but at different cost.

4.3 Case study 3: The Escherichia coli K-12 transcriptional motif

Input The full weighted ADMG in Fig. 7 (a) is a transcriptional regulatory network motif of *E. Coli*. The network was obtained from the EcoCyc database Keseler et al. [2021]. All the weights were set to 1. The query of interest is $Q_{fur} = P(dpiA|do(fur = 0))$. $\mathbb{W} = \infty$, and $N = 262$.

Step 1: Simulating future data sets We used 262 RNA-seq normalized expression profiles of *E. Coli* K-12 MG1655 and BW25113 across 154 unique experimental conditions from the PRECISE database [Sastry et al., 2019]. The dataset also included interventional data with $fur = 0$. It was used to evaluate the accuracy of the estimators. Based on these historical data, we generated two synthetic datasets. The first was generated from a Bayesian Network, trained on the experimental data using parametrized generalized linear models (GLMs). At each node the GLMs had a Normal or Gamma distribution with identity/log link functions. Bayesian Information Criterion (BIC) was used to guide feature engineering/transformations. Once the model was trained, new samples were generated by forward simulation. The second synthetic dataset was generated from Tabular GAN Xu et al. [2019]. We preprocessed the data as described in Ashrapov [2020] with default hyperparameters.

Step 2: Exploring sub-ADMGs The adjustment set are the olive nodes in Fig. 7 excluding the treatment and effect. Selected sub-ADMGs from the whole set of sub-ADMGs are shown in Fig. 7 (c)-(e) with their corresponding measurement costs. Fig. 7 (b) shows the simplified ADMG of the full network in Fig. 7 (a) where the gray, and red nodes are removed. Sub-ADMG in Fig. 7 (c) only consist of the treatment, effect, and the adjustment set. Sub-ADMG in Fig. 7 (d) contains a single mediator. Sub-ADMG in Fig. 7 (e) contains all the mediators.

Step 3: Estimating causal query Since the treatment fur was continuous, we considered the causal generative and linear regression estimators.

Output and conclusions Fig. 7 (f) summarizes the queries estimated over $K = 100$ simulated observational data sets. We can make several conclusions. 1) Since causal generative model did not use all the input nodes, using the full network in Fig. 7(a) had the exact same result as in Fig. 7(b) and (e). However, the full network had a larger cost. 2) For linear regression, using the full network in Fig. 7(a) increased the variance and slightly biased the results as compared to most other sub-ADMGs. 3) Compared to only using the treatment, effect and adjustment set (olive nodes) in Fig. 7(c), including a single mediator (Fig. 7 (d)) reduced the variance by over 50% for most estimators; 4) Including all the mediators (Fig. 7(e) slightly decreased the variance compared to the subnetwork with a single mediator in Fig. 7(d), but at extra cost; 5) Different simulation strategies lead to same ranking of sub-ADMGs, but with different variances.

4.4 Summary of the conclusions of the Case studies

Expanding the set of measured variables beyond the adjustment was beneficial in presence of mediators. Lemma 1 stated theoretically, and all the case studies showed empirically, that expanding the adjustment set with at least one mediator reduced the variance of the causal query estimator. The benefits of including multiple mediators were Case study-specific.

Measuring a subset of the variables was often more effective than measuring the entire network. In illustrative example and Case study 3, using all the variables biased the causal query estimator. In Case studies 1 and 2, well-chosen subsets of variables resulted in similar or smaller variances of the estimators, but at lower cost.

Experimental design depended on the choice of the query estimation method. The different restrictions on the input variables, and the different functional forms of the estimators impacted the variances associated with subsets of variables, as illustrated in Case studies 1 and 2.

Experimental design depended on the sample size. The sample size N affected the relative performance of the subsets of variables and of the estimators in Case study 1.

5 Discussion

We proposed an approach for selecting optimal subsets of variables, to quantify in future observational studies with the purpose of causal query estimation. A limitation of the proposed approach is the requirement of a known biomolecular

network. We overcame this limitation in part by working with ADMGs, which allow us to misspecify the latent variables as long as the observed variables are represented accurately. The correctness of the structure over observed variables can be checked with the falsification module in Y_0 Zucker and Hoyt [2021]. Another potential limitation is the accuracy of the generated synthetic data, which can be addressed by sensitivity analysis. Finally, although the estimators supported by the proposed approach are (asymptotically) unbiased, they may be biased in practice. This is due to violations of model assumptions, and to the relatively small sample size. Simulating interventional data, as in the Case studies in this manuscript, helps diagnose and account for this issue in the choice of a sub-ADMG.

Future directions of this research include a closer integration with simulated interventional data. This will allow us to expand the scope of causal queries, check their identifiability, e.g. with the G-ID algorithm Lee et al. [2020], and increase their practical use.

Funding

JZ is supported by the PNNL Directed R&D-funded Data-Model Convergence Initiative. PNNL is operated for the DOE by Battelle Memorial Institute under Contract DE-AC05-76RLO1830. CTH is supported by the DARPA Young Faculty Award W911NF2010255 (PI: Benjamin M. Gyori). KS is supported by Muscular Dystrophy Association MDA Award #574137. OV acknowledges the support of NSF-BIO/DBI 1759736, NSF-BIO/DBI 1950412, NIH-NLM-R01 1R01LM013115 and of the Chan-Zuckerberg foundation.

References

- Judea Pearl. *Causality*. Cambridge university press, 2009.
- Yonghan Jung, Jin Tian, and Elias Bareinboim. Learning causal effects via weighted empirical risk minimization. *Advances in Neural Information Processing Systems*, 33, 2020a.
- Yonghan Jung, Jin Tian, and Elias Bareinboim. Estimating causal effects using weighting-based estimators. In *AAAI*, page 10186, 2020b.
- Rohit Bhattacharya, Razieh Nabi, and Ilya Shpitser. Semiparametric inference for causal effects in graphical models with hidden variables. *arXiv:2003.12659*, 2020.
- John A Bachman, Benjamin M Gyori, and Peter K Sorger. Automated assembly of molecular mechanisms at scale from text mining and curated databases. *bioRxiv*, 2022.
- Marc Gillespie, Bijay Jassal, Ralf Stephan, Marija Milacic, Karen Rothfels, Andrea Senff-Ribeiro, Johannes Griss, Cristoffer Sevilla, Lisa Matthews, Chuqiao Gong, et al. The reactome pathway knowledgebase 2022. *Nucleic Acids Research*, 50:D687, 2022.
- Dénes Túrei, Tamás Korcsmáros, and Julio Saez-Rodriguez. OmniPath: guidelines and gateway for literature-curated signaling pathway resources. *Nature Methods*, 13:966, 2016.
- Carlos Cinelli, Andrew Forney, and Judea Pearl. A Crash Course in Good and Bad Controls. *Available at SSRN 3689437*, 2020.
- Andrea Rotnitzky and Ezequiel Smucler. Efficient adjustment sets for population average causal treatment effect estimation in graphical models. *Journal of Machine Learning Research*, 21, 2020.
- Leonard Henckel, Emilija Perković, and Marloes H Maathuis. Graphical criteria for efficient total effect estimation via adjustment in causal linear models. *arXiv:1907.02435*, 2019.
- Jakob Runge. Necessary and sufficient graphical conditions for optimal adjustment sets in causal graphical models with hidden variables. *Advances in Neural Information Processing Systems*, 34:15762, 2021.
- Yue Cao, Pengyi Yang, and Jean Yee Hwa Yang. A benchmark study of simulation methods for single-cell RNA sequencing data. *Nature Communications*, 12:1, 2021.
- Mohamed Marouf, Pierre Machart, Vikas Bansal, Christoph Kilian, Daniel S Magruder, Christian F Krebs, and Stefan Bonn. Realistic in silico generation and augmentation of single-cell RNA-seq data using generative adversarial networks. *Nature Communications*, 11:1, 2020.
- Tianyi Sun, Dongyuan Song, Wei Vivian Li, and Jingyi Jessica Li. scDesign2: a transparent simulator that generates high-fidelity single-cell gene expression count data with gene correlations captured. *Genome Biology*, 22:1, 2021.
- Luca Marchetti, Corrado Priami, and Vo Hong Thanh. Stochastic simulation of biochemical reaction systems. In *Simulation Algorithms for Computational Systems Biology*, page 7. 2017.

- Stephan Schmeing and Mark D Robinson. ReSeq simulates realistic Illumina high-throughput sequencing data. *Genome Biology*, 22:1, 2021.
- Bo Peng, Huann-Sheng Chen, Leah E Mechanic, Ben Racine, John Clarke, Elizabeth Gillanders, and Eric J Feuer. Genetic data simulators and their applications: an overview. *Genetic Epidemiology*, 39:2, 2015.
- Fabian Dunke and Stefan Nickel. Simulation-based multi-criteria decision making: an interactive method with a case study on infectious disease epidemics. *Annals of Operations Research*, page 1, 2021.
- Peter Spirtes, Clark N Glymour, Richard Scheines, and David Heckerman. *Causation, Prediction, and Search*. 2000.
- Frederick Eberhardt and Richard Scheines. Interventions and causal inference. *Philosophy of Science*, 74:981, 2007.
- Guido W Imbens and Donald B Rubin. *Causal inference in Statistics, Social, and Biomedical Sciences*. 2015.
- Thomas S. Richardson, Robin J. Evans, James M. Robins, and Ilya Shpitser. Nested Markov properties for acyclic directed mixed graphs. *arXiv*, 2017.
- Robin J Evans. Graphs for margins of Bayesian networks. *Scandinavian Journal of Statistics*, 43:625–648, 2016.
- Markus Kalisch, Martin Mächler, Diego Colombo, Marloes H Maathuis, and Peter Bühlmann. Causal inference using graphical models with the R package pcalg. *Journal of Statistical Software*, 47:1, 2012.
- Johannes Textor, Benito Van der Zander, Mark S Gilthorpe, Maciej Liśkiewicz, and George TH Ellison. Robust causal inference using directed acyclic graphs: the R package ?dagitty? *International Journal of Epidemiology*, 45:1887, 2016.
- Santtu Tikka and Juha Karvanen. Identifying Causal Effects with the R Package causaleffect. *Journal of Statistical Software*, 76:1, 2017.
- Jinyong Hahn. Functional restriction and efficiency in causal inference. *The Review of Economics and Statistics*, 86:73, 2004.
- Halbert White and Xun Lu. Causal diagrams for treatment effect estimation with application to efficient covariate selection. *Review of Economics and Statistics*, 93:1453, 2011.
- Amit Sharma, Emre Kiciman, et al. DoWhy: A Python package for causal inference.
- Jeremy Zucker and Charles Hoyt. Y_0 Causal Inference Engine. <https://y0.readthedocs.io/en/latest/>, 2021.
- Sara Mohammad-Taheri, Jeremy Zucker, Charles Tapley Hoyt, Karen Sachs, Vartika Tewari, Robert Ness, and Olga Vitek. Do-calculus enables estimation of causal effects in partially observed biomolecular pathways. *Bioinformatics*, 38:350, 2022.
- Marc F Bellemare, Jeffrey R Bloem, and Noah Wexler. The paper of how: Estimating treatment effects using the front-door criterion. Technical report, 2019.
- Ian Goodfellow, Jean Pouget-Abadie, Mehdi Mirza, Bing Xu, David Warde-Farley, Sherjil Ozair, Aaron Courville, and Yoshua Bengio. Generative adversarial networks. *Communications of the ACM*, 63:139, 2020.
- Burak Yelmen, Aurelien Decelle, Linda Ongaro, Davide Marnetto, Corentin Tallec, Francesco Montinaro, Cyril Furtlehner, Luca Pagani, and Flora Jay. Creating artificial human genomes using generative models. *bioRxiv*, page 769091, 2019.
- Nick Pawlowski, Daniel Coelho de Castro, and Ben Glocker. Deep structural causal models for tractable counterfactual inference. *Advances in Neural Information Processing Systems*, 33:857, 2020.
- Edward Choi, Siddharth Biswal, Bradley Malin, Jon Duke, Walter F Stewart, and Jimeng Sun. Generating multi-label discrete patient records using generative adversarial networks. In *Machine Learning for Healthcare Conference*, page 286, 2017.
- John Weldon, Tomas Ward, and Eoin Brophy. Generation of synthetic electronic health records using a federated GAN. *arXiv:2109.02543*, 2021.
- Lei Xu, Maria Skoularidou, Alfredo Cuesta-Infante, and Kalyan Veeramachaneni. Modeling tabular data using conditional gan. *Advances in Neural Information Processing Systems*, 32, 2019.
- Daphne Koller and Nir Friedman. *Probabilistic Graphical Models: Principles and Techniques*. 2009.
- Uri Alon. *An Introduction to Systems Biology: Design Principles of Biological Circuits*. 2019.
- Stan Development Team. RStan: the R interface to Stan, 2020. R package version 2.21.2.
- D. T. Gillespie. Exact stochastic simulation of coupled chemical reactions. *Journal of Physical Chemistry*, 81:2340, 1977.
- Darren Wilkinson, Maintainer Darren Wilkinson, and Suggests deSolve. Package ?smfsb? 2018.

- Z. S. Ulhaq and G. V. Soraya. Interleukin-6 as a potential biomarker of COVID-19 progression. *Medecine et Maladies Infectieuses*, 50:382, 2020.
- T. Hirano and M. Murakami. COVID-19: A new virus, but a familiar receptor and cytokine release syndrome. *Immunity*, 52:731, 2020.
- Ingrid M Keseler, Socorro Gama-Castro, Amanda Mackie, Richard Billington, César Bonavides-Martínez, Ron Caspi, Anamika Kothari, Markus Krummenacker, Peter E Midford, Luis Muñoz-Rascado, et al. The EcoCyc database in 2021. *Frontiers in Microbiology*, page 2098, 2021.
- Anand V Sastry, Ye Gao, Richard Szubin, Ying Hefner, Sibe Xu, Donghyuk Kim, Kumari Sonal Choudhary, Laurence Yang, Zachary A King, and Bernhard O Palsson. The *Escherichia coli* transcriptome mostly consists of independently regulated modules. *Nature Communications*, 10:1, 2019.
- Insaf Ashrapov. Tabular GANs for uneven distribution. *arXiv:2010.00638*, 2020.
- Sanghack Lee, Juan D. Correa, and Elias Bareinboim. General identifiability with arbitrary surrogate experiments. In *Proceedings of The 35th Uncertainty in Artificial Intelligence Conference*, page 389, 2020.

Appendix

A Algorithms

We provide details of the functions used in Algo 1.

Algo 2 takes as input an ADMG, treatment, effect, and the upper limit on the total weight and outputs a valid adjustment set with minimum weight such that its total cost does not exceed the upper limit total weight and it contains all the good neutral controls.

Algo 3 takes as input a set of weighted nodes and produces their powerset conditioned on having sum of weights in each subset to be less than a given threshold. The subsets are recursively constructed by calling Algo 4.

Algo 5 takes as input an ADMG, and the set of variables that the experimenter decides to measure, and it outputs the corresponding sub-ADMG that contains only the new measure set by applying the simplification rules in Sec. 2.1.

Algorithm 2: generateValidAdjustmentSet

Input: $\mathcal{G} = (\mathbf{V}, \mathbf{E}_d, \mathbf{E}_b, \mathbf{W})$: Weighted ADMG

T, Y : Treatment and effect

\mathbb{W} : Upper limit on the total weight

Output: Valid adjustment set with minimum weight that includes the variables that possibly decrease the variance of the query estimator (good neutral controls)

```

// All valid adjustment sets from the dagitty software
1 A = adjustmentSets( $\mathcal{G}, T, Y$ )
2 minAdjSetCost = Inf
3 selectedAdjustmentSet = {}
4 forbiddenSet =  $de(cp(T, Y, \mathcal{G})) \cup T$ 
// Good neutral control set
5 gnControlSet =  $Pa(cp(T, Y, \mathcal{G})) \setminus forbiddenSet$ 
6 for  $a \in \mathbf{A}$  do
7    $\mathbb{W}_a = \text{sumWeights}(a)$ 
8   if  $\mathbb{W}_a > \mathbb{W}$  then
9     continue
10  end
11  if  $\mathbb{W}_a < \text{minAdjSetCost}$  and  $a \subseteq gnControlSet$  then
12    minAdjSetCost =  $\mathbb{W}_a$ 
13    selectedAdjustmentSet =  $a$ 
14  end
15 end
16 return selectedAdjustmentSet

```

Algorithm 3: getValidNodeSubsets

Input: $\mathcal{G} = (\mathbf{V}, \mathbf{E}_d, \mathbf{E}_b, \mathbf{W})$: Weighted ADMG

A : A valid adjustment set

T, Y : Treatment and effect

\mathbb{W} : Upper limit on the total weight

Output: Subsets of nodes in the given ADMG which has sum of weights less than or equal to \mathbb{W} and also include T, Y , and the nodes in A .

```

1 requiredNodes  $\leftarrow \mathbf{A} \cup T \cup Y$  //Olive nodes
2 optionalNodes  $\leftarrow \mathbf{V} \setminus \{requiredNodes\}$  //Yellow and green nodes
3 result = []
// Recursively add subsets to the result.
4 getValidNodeSubsetsHelper(requiredNodes, optionalNodes,  $\mathbb{W}, 0, [], \text{result}$ )
5 return result

```

Algorithm 4: getValidNodeSubsetsHelper

Input: requiredNodes : Set of nodes present in each subset
 optionalNodes: Set of optional nodes in a subset
 \mathbb{W} : Total weight limit
 idx: Current index
 subset: Current subset
 result: Power set

Output: Recursively adds subsets of optionalNodes to the result. requiredNodes are also added to each subset.

```

1 if  $sum(subset.weight) + sum(requiredNodes.weight) > \mathbb{W}$  then
2   | return
3 end
4 if  $idx == optionalNodes.length$  then
5   | subset.add(requiredNodes)
6   | result.add(subset)
7 end
8 getValidNodeSubsetsHelper(requiredNodes, optionalNodes,  $\mathbb{W}$ , idx+1, subset.copy(), result)
9 subset.add(optionalNodes[idx])
10 generateValidSubsetsHelper(requiredNodes, optionalNodes,  $\mathbb{W}$ , idx+1, subset.copy(), result)

```

Algorithm 5: generateSubADMG

Input: $\mathcal{G} = (\mathbf{V}, \mathbf{E}_d, \mathbf{E}_b)$: ADMG,
 $\mathbf{V}' \subseteq \mathbf{V}$: new Measure set ,

Output: Sub-ADMG where the observed nodes are changed to \mathbf{V}' and new latent nodes are added to the current set of latent nodes.

```

1  $\mathbf{U} = \mathbf{V} \setminus \mathbf{V}'$ 
  // Apply simplification rules in Sec. 2.1
2  $\mathcal{G}' = \text{simplifiedNetwork}(\mathcal{G}, \mathbf{U})$ 
3 return  $\mathcal{G}'$ 

```

Figure	Formula
Fig. 5 (a)	$Raf = \beta_0 + \beta_1 AKT + \beta_2 PI3K + \beta_3 Ras + \beta_4 SOS + \varepsilon_1$ $Mek = \beta_5 + \beta_6 Raf + \beta_7 AKT + \beta_8 PI3K + \beta_9 Ras + \beta_{10} SOS + \varepsilon_2$ $Erk = \beta_{11} + \beta_{12} Mek + \beta_{13} Raf + \beta_{14} AKT + \beta_{15} Ras + \beta_{16} PI3K + \beta_{17} SOS + \varepsilon_3$
Fig. 5 (b)	$Erk = \beta_{18} + \beta_{19} AKT + \beta_{20} PI3K + \varepsilon_4$
Fig. 5 (c)	$Mek = \beta_{21} + \beta_{22} AKT + \beta_{23} PI3K + \varepsilon_5$ $Erk = \beta_{24} + \beta_{25} Mek + \varepsilon_6$
Fig. 5 (d)	$Erk = \beta_{26} + \beta_{27} AKT + \beta_{28} SOS + \beta_{29} PI3K + \varepsilon_7$

Table 2: **Case study 1. Formulas used to estimate the query** $E[Erk|do(Akt = 80)]$. The error terms $(\varepsilon_1, \dots, \varepsilon_7)$ are *i.i.d* and follow $\mathcal{N}(0, \sigma_i^2)$ for $i \in \{1, \dots, 7\}$

B Including mediators into estimation of causal query reduce the asymptotic variance

Lemma 1 Consider an ADMG A , where T is the target of intervention and Y is the effect. Including the mediators in any statistical estimator results in less variance than not including any of them.

Proof. First, assume that there is only a single mediator M_1 . The chain rule for mutual information implies that

$$I(T, M_1; Y) = I(T; Y) + I(M_1; Y|T) \quad (14)$$

The mutual information is non-negative. This implies that $I(T, M_1; Y) > I(T; Y)$, i.e., the amount of information obtained about Y by observing both T and M_1 is more than the amount of information obtained about Y by observing only T . A higher mutual information value indicates a larger reduction of uncertainty whereas a lower value indicates a smaller reduction. Hence, measuring M_1 helps to reduce the uncertainty about Y , and it reduces its variation.

Next, we extend this property to multiple mediators, M_1, \dots, M_k . Expanding the chain rule for all the mediators,

$$I(T, M_1, \dots, M_k; Y) = I(T; Y) + I(M_1; Y|T) + \sum_{i=2}^k I(M_i; Y|T, M_1, \dots, M_{i-1})$$

Following the same logic as above, $I(T, M_1, \dots, M_k; Y) > I(T; Y)$, i.e., the amount of information obtained about Y by observing both T and M_1, \dots, M_k , exceeds the amount of information obtained about Y by observing only T . \square

Lemma 1 implies that including all or a subset of the mediators improves the precision of the query estimation.

Causal query estimation details of the Case studies

Case study 1 For the causal generative approach, we modeled the exogenous variables with a Gaussian distribution. The rest of the variables were modeled by representing the biomolecular reactions with a Hill function as described in Case study 2, Step 1. The non-informative $\mathcal{N}(0, 10)$ priors were used for the parameters θ in the sigmoid function. The linear regression in Fig. 5 used the equations in Table 2.

Case study 2 For the semi-and non-parametric approaches we directly used the Ananke library Bhattacharya et al. [2020]. For the linear regression approach we used the equations in Table 3.

Case study 3 For the causal generative approach, we modeled the variables as in the causal generative approach in Case study 1. For the linear regression approach, we used the equations in Table 4.

Figure	Formula
Fig. 6 (a)	$NFKB = \gamma_0 + \gamma_1 EGFR + \gamma_2 ADAM17 + \gamma_3 TNF + \gamma_4 SARSCOV2$ $+ \gamma_5 ACE2 + \gamma_6 Ang + \gamma_7 AGTR1 + \gamma_8 Gefi + \gamma_9 PRR + \epsilon_1$ $IL6AMP = \gamma_{10} + \gamma_{11} NFKB + \gamma_{12} IL6STAT3 + \gamma_{13} ACE2 + \gamma_{14} ADAM17$ $+ \gamma_{15} TNF + \gamma_{16} EGFR + \gamma_{17} Toci + \gamma_{18} Gefi + \gamma_{19} PRR + \epsilon_2$ $cytok = \gamma_{20} + \gamma_{21} IL6AMP + \gamma_{22} SARSCOV2 + \gamma_{23} ACE2 + \gamma_{24} Ang$ $+ \gamma_{25} AGTR1 + \gamma_{26} Sil6r + \gamma_{28} TNF + \gamma_{29} NFKB + \gamma_{30} Gefi + \epsilon_3$
Fig. 6 (b)	$cytok = \gamma_{31} + \gamma_{32} EGFR + \gamma_{33} ADAM17 + \gamma_{34} TNF$ $+ \gamma_{35} Sil6r + \gamma_{36} IL6STAT3 + \epsilon_4$
Fig. 6 (c)	$cytok = \gamma_{37} + \gamma_{38} EGFR + \gamma_{39} ADAM17 + \gamma_{40} TNF + \gamma_{41} sIL6R\alpha$ $+ \gamma_{42} IL6STAT3 + \gamma_{43} Gefi + \gamma_{44} EGF + \epsilon_5$
Fig. 6 (d)	$NFKB = \gamma_{45} + \gamma_{46} EGFR + \gamma_{47} ADAM17 + \gamma_{47} TNF$ $+ \gamma_{48} ACE2 + \gamma_{49} Gefi + \epsilon_6$ $IL6AMP = \gamma_{50} + \gamma_{51} NFKB + \gamma_{52} IL6STAT3 + \gamma_{53} ACE2 + \gamma_{54} ADAM17$ $+ \gamma_{55} TNF + \gamma_{56} EGFR + \gamma_{57} Gefi + \gamma_{58} PRR + \epsilon_7$ $cytok = \gamma_{59} + \gamma_{60} IL6AMP + \gamma_{61} ACE2 + \gamma_{62} Sil6r$ $+ \gamma_{63} TNF + \gamma_{64} NFKB + \gamma_{65} Gefi + \epsilon_8$

Table 3: **Case study 2. Formulas used to estimate the ATE.** The error terms $(\epsilon_1, \dots, \epsilon_8)$ are *i.i.d* and follow $\mathcal{N}(0, \sigma_i^2)$ for $i \in \{1, \dots, 8\}$

Figure	Formula
Fig. 7 (a)	$dpiA = \phi_0 + \phi_1 fnr + \phi_2 crp + \phi_3 rpoD + \phi_4 oxyR + \phi_5 dcuR + \phi_6 narL + \phi_7 fur$ $+ \phi_8 aspC + \phi_9 dpiB + \phi_{10} hyaA + \phi_{11} appY + \phi_{12} hyaB + \phi_{13} hyaF + \epsilon_1$ $fnr = \phi_{14} + \phi_{15} fur + \phi_{16} rpoD + \phi_{17} crp + \epsilon_2$
Fig. 7 (b)	$dpiA = \phi_{18} + \phi_{19} fnr + \phi_{20} crp + \phi_{21} rpoD + \phi_{22} oxyR + \phi_{23} dcuR + \phi_{24} narL + \phi_{25} fur + \epsilon_3$ $fnr = \phi_{26} + \phi_{27} fur + \phi_{28} rpoD + \epsilon_4$
Fig. 7 (c)	$dpiA = \phi_{29} + \phi_{30} fur + \phi_{31} crp + \phi_{32} rpoD + \epsilon_5$
Fig. 7 (d)	$dpiA = \phi_{33} + \phi_{34} fnr + \phi_{35} fur + \phi_{36} rpoD + \phi_{37} dcuR + \phi_{38} crp + \epsilon_6$ $fnr = \phi_{39} + \phi_{40} fur + \phi_{41} rpoD + \phi_{42} crp + \epsilon_7$
Fig. 7 (e)	$dpiA = \phi_{43} + \phi_{44} fnr + \phi_{45} fur + \phi_{46} rpoD + \phi_{47} dcuR + \phi_{48} narL + \phi_{49} crp + \epsilon_8$ $fnr = \phi_{50} + \phi_{51} fur + \phi_{52} rpoD + \epsilon_9$

Table 4: **Case study 3. Formulas used to estimate the query $E[dpiA|do(fur = 0)]$.** The error terms $(\epsilon_1, \dots, \epsilon_9)$ are *i.i.d* and follow $\mathcal{N}(0, \sigma_i^2)$ for $i \in \{1, \dots, 9\}$.